Impulse Resistance of Concentrated Tower Grounding Systems Simulated by an ATPDraw Object

Z. G. Datsios, P. N. Mikropoulos, T. E. Tsovilis

Abstract--**Tower grounding system accurate modeling is very important in evaluating the backflashover surges arising at overhead transmission lines and impinging on the connected substations. A new ATPDraw object, called TGIR, has been developed with the aid of which a concentrated tower grounding system can be represented on the basis of several tower grounding system models. The TGIR object was employed in ATP-EMTP simulations of a 150 kV GIS substation. The computed backflashover surges impinging on the substation vary considerably among the tower grounding system models employed in simulations, as a result of the variability in the grounding impulse resistance. The TGIR object is a useful tool within the ATP-EMTP environment for insulation co-ordination studies; the effects of tower grounding system modeling on backflashover surges arising at overhead transmission lines and impinging on the connected substations can be easily quantified.**

***Keywords*: ATP-EMTP, ATPDraw, concentrated tower grounding system, GIS substation, insulation co-ordination, lightning surges, MODELS, overhead transmission lines.**

I. Introduction

BACKFLASHOVER, that is line insulation flashover due to lightning strokes to shield wires, is one of the main causes of transmission line outages and may also result in substation outages, caused by incoming surges with amplitude exceeding the insulation level of substation equipment. Backflashover is associated with the overvoltages arising across the transmission line insulator strings owing to the increase of the tower potential when lightning strokes are intercepted by shield wires. These overvoltages are greatly determined by the transmission line tower grounding system. Hence, modeling of the latter is important for evaluating the backflashover surges arising at the overhead transmission line, thus also, incoming to the connected substations.

Depending on the grounding electrode dimensions, tower grounding systems can be categorized as concentrated or extended. Most commonly, for fast-front transient studies, a concentrated tower grounding system is modeled as either a constant resistance [1]-[3] or a current-dependent resistance, when considering the reduction of the tower footing resistance due to soil ionization [4]-[11].

In this study, a new ATPDraw [12] object is presented yielding the grounding impulse resistance of a concentrated tower grounding system on the basis of several models reported in literature. The new object, called TGIR, has been developed by using MODELS language [13], [14]. The TGIR object has been applied to simulate the grounding system of a typical 150 kV tower of the Hellenic transmission system and to evaluate the computed backflashover surges impinging on a 150 kV GIS substation with respect to the tower grounding system model adopted. The computed overvoltages vary significantly in terms of both amplitude and waveshape among the tower grounding system models employed in simulations. This results from the variability in the grounding impulse resistance among models and has been easily quantified with the aid of the new ATPDraw object.

II. Models of Concentrated Tower Grounding Systems

Tower grounding systems can be considered as concentrated when grounding electrodes with relatively small dimensions cover distances shorter than 30 m from the tower base [9], [15]. For fast-front transient studies, a concentrated tower grounding system can be modeled as a constant resistance with value equal to either the power frequency resistance [1] or 10 Ω as recommended in [2] for system voltage higher than 77 kV or a surge-reduced constant resistance taking into account a surge reduction curve in order to consider soil ionization [3]. In addition, a concentrated tower grounding system can be modeled more accurately as a current-dependent resistance [4]-[11], considering, thus, the decrease of the tower footing impedance to values lower than the initial low current and low frequency grounding resistance due to soil ionization.

According to the concentrated tower grounding system models [4]-[8], which are all based on the similarity theory, the tower footing impedance is described in terms of two dimensionless parameters, Π_1 and Π_2 as given by (1) and (2), respectively. Several curves correlating Π_1 and Π_2 have been proposed based on a large number of experimental results for grounding electrodes with different dimensions and shape and for different soil conditions (Table I).

In (1) and (2) $R(I)$ is the current-dependent tower footing resistance in Ω, s (m) is the characteristic dimension of the

---

Z. G. Datsios, P. N. Mikropoulos and T. E. Tsovilis are with the High Voltage Laboratory, Department of Electrical Energy, School of Electrical and Computer Engineering, Faculty of Engineering, Aristotle University of Thessaloniki, Thessaloniki 54124 Greece. (e-mail: zdatsios@auth.gr, pnm@eng.auth.gr, tsovilis@ee.auth.gr).

Paper submitted to the International Conference on Power Systems Transients (IPST2011) in Delft, the Netherlands June 14-17, 2011

TABLE I
DIMENSIONLESS PARAMETERS Π_1 AND Π_2

Model	Expression
Adapted from Korsuntsev [4]	$\Pi_1 = 0.2564 \cdot \Pi_2^{-0.3341}$, $0.03 \le \Pi_2 \le 5$ $\Pi_1 = 0.3367 \cdot \Pi_2^{-0.4927}$, $5 < \Pi_2 \le 100$
Oettle [6]	$\log \Pi_1 = -0.3 \cdot \log \Pi_2 - 0.62$ $\log \Pi_1 = -0.3 \cdot \log \Pi_2 - 0.49$ * $0.005 \le \Pi_2 \le 20$
Chisholm et al. [7] from Popolansky [5]	$\Pi_1 = 0.2631 \cdot \Pi_2^{-0.3082}$, $0.3 \le \Pi_2 \le 10$
Chowdhuri [8] from Popolansky [5]	$\Pi_1 = 0.2965 \cdot \Pi_2^{-0.2867}$, $\Pi_2 \le 5$ $\Pi_1 = 0.4602 \cdot \Pi_2^{-0.6009}$, $5 < \Pi_2 \le 50$ $\Pi_1 = 0.9534 \cdot \Pi_2^{-0.7536}$, $50 < \Pi_2 \le 500$ $\Pi_1 = 1.8862 \cdot \Pi_2^{-0.8693}$, $\Pi_2 > 500$

* conservative estimation

$$\Pi_1 = \frac{R(I) \cdot s}{\rho} \tag{1}$$

$$\Pi_2 = \frac{I \cdot \rho}{s^2 \cdot E_0} \tag{2}$$

grounding electrode, which is defined as the distance from the the geometric center of the electrode on the ground surface to the outermost point of the electrode, ρ (Ωm) is the soil resistivity, E_0 (kV/m) is the critical soil ionization gradient and I (kA) is the current flowing through the grounding system.

Oettle [6], to account for three-dimensional types of grounding electrodes defined the characteristic dimension as

$$s = \sqrt{d_1^2 + d_2^2 + d^2} \tag{3}$$

where d_1 (m) is largest horizontal distance of the electrode, d_2 (m) is the horizontal dimension which lies perpendicular to the largest horizontal distance and d (m) is the burial depth.

Chisholm et al. model [7] incorporates the experimental curve relating Π_1 and Π_2 from Popolansky [5] to estimate the resistive response of the grounding system, $R(I)$, and considers also the surge response of a ground plane. Thus, the tower footing impedance, $R_f(I)$, is given in Ω as

$$R_f(I) = R(I) + L_f / t_f \tag{4}$$

where L_f (μH) is the tower footing inductance, given by (5), corresponding to the inductive component of the grounding electrode surge response and t_f (μs) is the front time of the lightning current. In (5) T_t (μs) is the tower travel time.

$$L_f = 60 \cdot T_t \cdot \ln\left(t_f / T_t\right) \tag{5}$$

CIGRE [9] adopted Weck's simplified concentrated tower grounding system model [10]; according to the latter, the tower grounding system is represented by a current-dependent tower footing resistance given as

$$R(I) = \frac{R_0}{\sqrt{1 + \dfrac{I}{I_g}}} \tag{6}$$

where R_0 (Ω) is the low current and low frequency resistance, I (kA) is the current flowing through the grounding system and I_g (kA) is the limiting current to initiate sufficient soil ionization expressed as

$$I_g = \frac{E_0 \cdot \rho}{2\pi \cdot R_0^2} \tag{7}$$

According to Yasuda et al. model [11], the current-dependent tower footing resistance, $R(I)$, is given by (8). In the latter, the limiting current I_g (kA) is given by (9), where r (m) is the equivalent radius of the tower footing and n is the number of footings per tower.

$$R(I) = \begin{cases} R_0, & I < I_g \\ \dfrac{R_0}{\sqrt{I/I_g}}, & I \ge I_g \end{cases} \tag{8}$$

$$I_g = \frac{2\pi r^2 n \cdot E_0}{\rho} \tag{9}$$

III. TGIR OBJECT

A new ATPDraw [12] object, called Tower Grounding Impulse Resistance (TGIR), has been developed by using MODELS language [13], [14] within the ATP-EMTP [16] environment. The TGIR object implements the concentrated tower grounding system models detailed above by incorporating a MODEL that controls a TACS Type 91 time-dependent resistor.

Fig. 1 shows the ATPDraw dialog box of the TGIR object; the user enters the input data, namely values for the low current and low frequency resistance (R0), soil resistivity (SR), critical soil ionization gradient (E0), characteristic dimension of the grounding system (S), number of footings per tower (N), equivalent radius of the tower footing (ER), front time of the lightning current (TF) and tower height (H). The user also selects the tower grounding system model to be used in simulations, by assigning a value to the parameter model selection (MS), ranging from 1 to 7 corresponding to the adopted grounding system model as numbered in Table II. This information on the input parameters is also provided in the help viewer window of the object.

The TGIR object was applied to simulate the grounding system of a typical 150 kV tower of the Hellenic transmission system. Fig. 2 shows the tower grounding impulse resistance

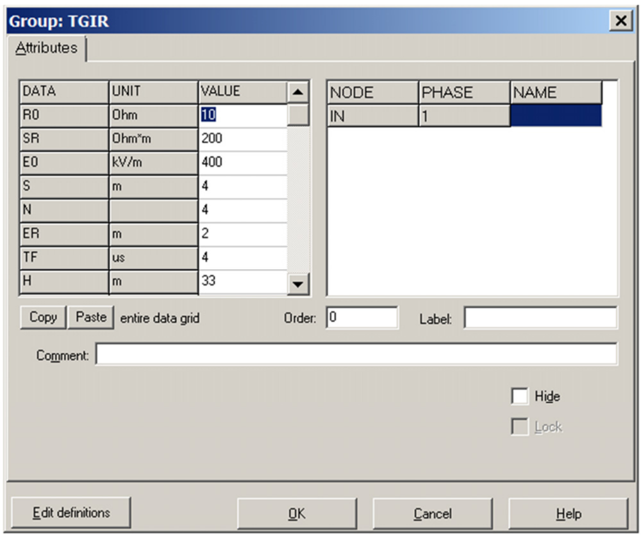

Fig. 1. ATPDraw input dialog box of the developed TGIR object.

TABLE II
CONCENTRATED GROUNDING SYSTEM MODELS PARAMETERS

No	Model	ρ (Ωm)	E_0 (kV/m)	s (m)
1	Korsuntsev [4]	200	1000*	4.56
2	Oettle [6]	200	1000	11.77
3	Chisholm et al. [7]	200	$241\cdot\rho^{0.215}$ or 1000**	4.56
4	Chowdhuri [8] from Popolansky [5]	200	1000*	4.56
5	CIGRE WG [9] from Weck [10]	200	300***	-
6	Yasuda et al. [11]	200	300***	-
7	Darveniza et al. [3]	-	-	-

* Proposed value for soil resistivity of 180 Ωm [4].
** Depending on model selection parameter of the TGIR object.
*** Proposed value according to [17].

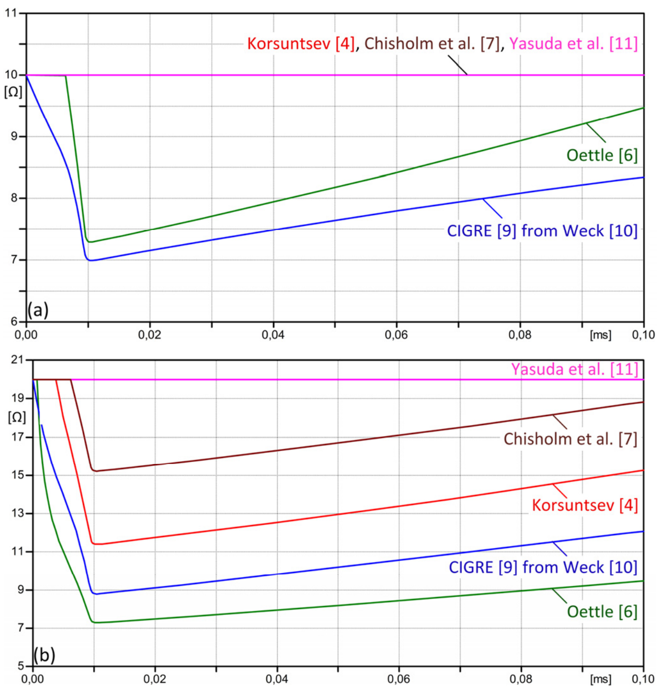

Fig. 2. Grounding system impulse resistance of a typical 150 kV tower of the Hellenic transmission system; lightning stroke current 100 kA, 6/77.5 μs, low current and low frequency grounding resistance (a) 10 Ω and (b) 20 Ω.

based on several tower grounding system models with parameters as given in Table II. In these simulations the lightning current flowing through the grounding system had an amplitude of 100 kA and a waveshape of 6/77.5 μs with front upwardly concave and maximum steepness according to [9]. From Fig. 2(a) it can be deduced that for relatively low values of power frequency resistance the tower grounding impulse resistance varies a little among models. However, this is not the case for relatively high values of power frequency resistance [Fig. 2(b)] and this may affect considerably the computed backflashover surges arising at the overhead transmission lines, thus also impinging on the connected substations. The latter is demonstrated in what follows.

IV. Application of the TGIR Object for the Evaluation of Backflashover Surges Impinging on Substations

The TGIR object was employed in ATP-EMTP [16] simulations for the evaluation of the backflashover surges impinging on a 150 kV GIS substation (Fig. 3). Simulations were performed for the following worst case scenario: negative lightning is assumed to strike to the top of the first tower (Fig. 4) close to the substation, at the time instant of positive power-frequency voltage peak of the upper phase of the overhead transmission line.

Lightning stroke was represented by a current source producing a current with an amplitude of 200 kA and a waveshape 8/77.5 μs with front upwardly concave and maximum steepness calculated according to [9]. The last section of the incoming overhead transmission line, 1.75 km in length, was represented by a sequence of J.Marti frequency-dependent models, considering the line span (350 m) and tower geometry (Fig. 4). Towers were modeled as vertical lossless single-phase frequency-independent distributed parameter lines with a surge impedance of 167 Ω calculated according to [1], [18]. Towers were terminated with the TGIR

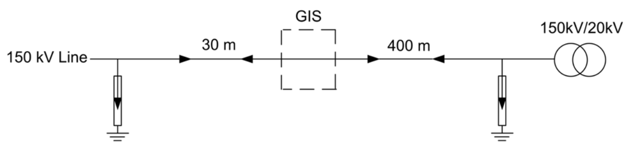

Fig. 3. Schematic diagram of the evaluated 150 kV GIS substation.

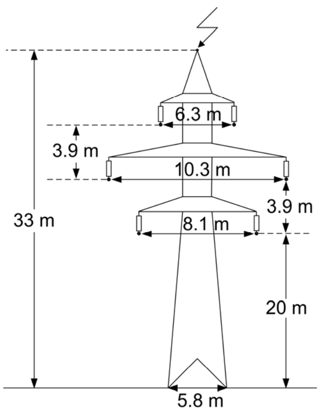

Fig. 4. Tower of a typical 150 kV double circuit overhead line of the Hellenic transmission system and lightning stroke location considered in simulations.

object by using a low current and low frequency resistance of 20 Ω and input values for the parameters required as shown in Table II. Transmission line insulator strings, with standard lightning impulse withstand voltage level of 750 kV and length of 1.86 m, were represented by voltage-dependent flashover switches controlled by a MODEL implementing Weck's leader development model [9], [15]. The underground XLPE power cables were represented by the Bergeron model with parameters calculated at 500 kHz. Surge arresters were represented by the Pinceti and Giannettoni frequency-dependent model [19] as shown in Fig. 5, with parameters calculated based on the surge arrester characteristics given in Table III. GIS bays were represented as lossless stub lines with a surge impedance of 75 Ω [15]. The step-up transformer was represented by a capacitance pi-circuit together with a BCTRAN model. Cable connections and the surge arrester lead lengths shorter than 3 m were modeled by a lumped parameter inductance of 1 μH/m [15]. Finally, simulations were performed with and without surge arresters operating at the line-cable junction so as to evaluate the protection offered against impinging surges with respect to the basic insulation level, BIL, of the GIS system (750 kV), considering also a safety factor of 1.15 [20].

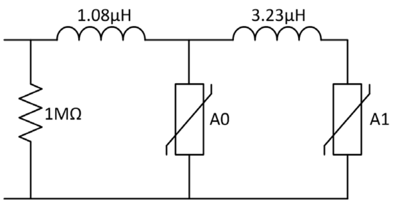

Fig. 5. Frequency-dependent surge arrester model [19]; parameters calculated based on the surge arrester characteristics given in Table III.

TABLE III
SURGE ARRESTER CHARACTERISTICS

System voltage	Rated voltage	Residual voltage 10 kA, 8/20 μs	Residual voltage 10 kA, 1/2 μs
150 kV	144 kV	346 kV	377 kV

Fig. 6(a) shows the computed overvoltages arising at the 150 kV GIS entrance using the tower grounding impulse resistance yielded by the TGIR object for several concentrated tower grounding system models, without surge arresters operating at the line-cable junction. The overvoltage, being dependent upon tower grounding impulse resistance, varies notably in terms of both peak and waveshape, among the tower grounding system models implemented in the TGIR object. However, from Fig. 6(b) it is obvious that this is less pronounced when surge arresters are operating at the line-cable junction according to common practice [21].

Fig. 7 summarizes the computed peak overvoltages arising at the 150 kV GIS entrance, obtained using the tower grounding impulse resistance yielded by the TGIR object. It is obvious that when surge arresters are not operating at the line-cable junction, the peak overvoltage varies significantly within the range of about 150% to 230% of the BIL of the GIS

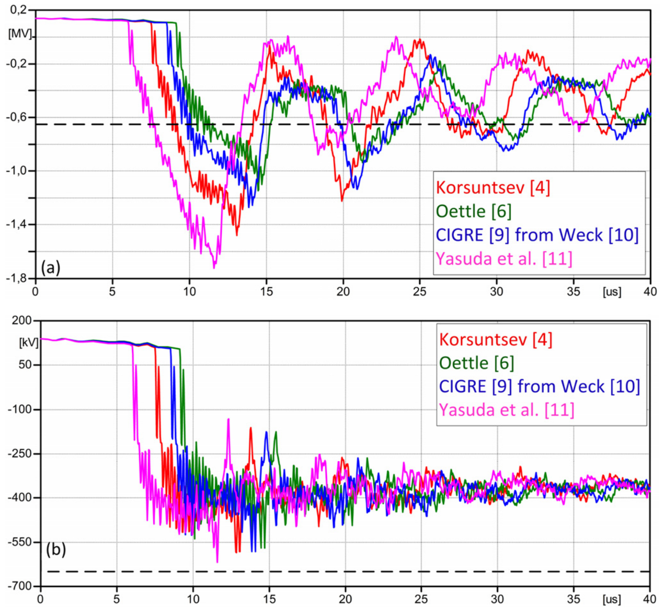

Fig. 6. Overvoltage at the entrance of the 150 kV GIS substation due to backflashover of the incoming line; dashed line depicts the safety margin of BIL/1.15, (a) and (b) without and with surge arresters operating at the line-cable junction, respectively.

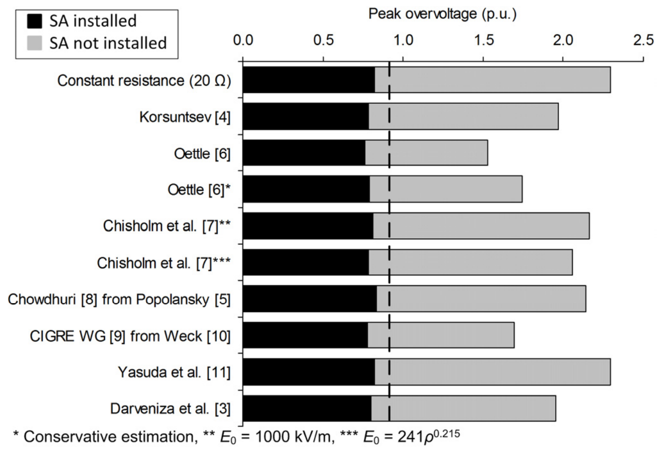

Fig. 7. Peak overvoltages arising at the entrance of the 150 kV GIS substation due to backflashover of the incoming line, with and without surge arresters operating at the line-cable junction; 1 p.u. = 750 kV, dashed line depicts the safety margin of BIL/1.15.

system (750 kV) among tower grounding system models. This is not the case when surge arresters are operating at the line-cable junction; the computed peak overvoltage varies lesser taking values lower than the BIL (<83%) of the 150 kV GIS system. It must be noted that differences in peak overvoltage among tower grounding system models are less pronounced for lower power frequency resistance [22]. Furthermore, from Fig. 7 it can be seen that representing the tower grounding system as a constant resistance with value equal to the power frequency tower footing resistance yields the highest peak overvoltage. This results in a safer design of the GIS substation in terms of the protection measures required against incoming backflashover surges.

Finally, in the present study, the TGIR object was used in ATP-EMTP to compute the backflashover surges impinging on the entrance of a GIS substation. It is well known that depending on substation layout, higher overvoltages may arise at other locations within GIS or along cables. These overvoltages would be also affected by tower grounding system modelling and this effect can be easily quantified with the aid of the TGIR object.

V. Conclusions

A new ATPDraw object, called TGIR, has been developed by using MODELS language. The TGIR object yields the grounding impulse resistance of a concentrated tower grounding system by considering the dimensions and power frequency resistance of the grounding system and the soil resistivity on the basis of several models reported in literature. The TGIR object enables the easy quantification of the differences in tower grounding impulse resistance among models; these differences are significant for relatively high values of power frequency tower footing resistance.

The TGIR object was employed in ATP-EMTP simulations of a 150 kV GIS substation. The computed backflashover surges impinging on the substation, being dependent upon tower grounding impulse resistance, vary in terms of both amplitude and waveshape among tower grounding system models. This is less pronounced when surge arresters are operating close to the substation entrance.

The TGIR object is a useful tool within the ATP-EMTP environment for utilities in assessing the backflashover surges arising at overhead transmission lines and impinging on the connected substations, as well as in selecting the necessary protection measures. The TGIR object can also be used for educational purposes in high voltage engineering courses and it is available at http://www.eng.auth.gr/hvl/.

VI. References

[1] IEEE Working Group, “A Simplified method for estimating lightning performance of transmission lines,” *IEEE Trans. Power App. Syst.*, vol. PAS-104, no. 4, pp. 919-932, Jul. 1985.

[2] A. Ametani and T. Kawamura, “A method of a lightning surge analysis recommended in Japan using EMTP,” *IEEE Trans. Power Del.*, vol. 20, no. 2, pp. 867-875, Apr. 2005.

[3] M. Darveniza, M. A. Sargent, G. J. Limbourn, Liew Ah Choy, R. O. Caldwell, J. R. Currie, B. C. Holcombe, R. H. Stillman, and R. Frowd, “Modelling for lightning performance calculations,” *IEEE Trans. Power App. Syst.*, vol. PAS-98, no. 6, pp. 1900-1908, Nov./Dec. 1979.

[4] A. V. Korsuntsev, “Application of the theory of similitude to the calculation of concentrated earth electrodes,” *Electrichestvo*, no.5, pp. 31-35, May 1958 (in Russian).

[5] F. Popolansky, “Determination of impulse characteristics of concentrated electrodes,” CIGRE SC 33-86 (WG 01) IWD 22, 1986.

[6] E. E. Oettle, “A new general estimation curve for predicting the impulse impedance of concentrated earth electrodes,” *IEEE Trans. Power Del.*, vol. 3, no. 4, pp 2020-2029, Oct. 1988.

[7] W. A. Chisholm and W. Janischewskyj, “Lightning surge response of ground electrodes,” *IEEE Trans. Power Del.*, vol. 4, no. 2, pp. 1329-1337, Apr. 1989.

[8] P. Chowdhuri, “Grounding for protection against lightning,” in Electromagnetic transients in power systems. Research Studies Press Ltd., John Wiley & sons inc., New York, 1996, pp. 104-113.

[9] CIGRE Working Group 33.01, “Guide to procedures for estimating the lightning performance of transmission lines,” Technical Bulletin 63, Oct. 1991.

[10] K. H. Weck, “The current dependence of tower footing resistance,” CIGRE 33-88 (WG01), 14 IWD, 1988.

[11] Y. Yasuda, Y. Hirakawa, K. Shiraishi, and T. Hara, “Sensitivity analysis on grounding models for 500kV transmission lines,” *Trans. IEE Japan B*, vol. 121, no. 10, pp. 1386-1393, 2001.

[12] L. Prikler and H. K. Høidalen, “ATPDRAW version 3.5 Users’ Manual”, SINTEF Energy Research, Norway, 2002.

[13] L. Dubé, “MODELS in ATP, language manual,” Feb. 1996.

[14] L. Dubé, “Users’ guide to MODELS in ATP,” Apr. 1996.

[15] IEEE Task Force, “Modeling guidelines for fast front transients,” *IEEE Trans. Power Del.*, vol. 11, no. 1, pp. 493-506, Jan. 1996.

[16] Canadian-American EMTP Users Group, “ATP Rule Book,” 1997.

[17] A. M. Mousa, “The soil ionization gradient associated with discharge of high currents into concentrated electrodes,” *IEEE Trans. Power Del.*, vol. 9, no. 3, pp. 1669-1677, Jul. 1994.

[18] M. A. Sargent and M. Darveniza, “Tower surge impedance,” *IEEE Trans. Power App. Syst.*, vol. PAS-88, no. 5, pp. 680-687, May 1969.

[19] P. Pinceti and M. Giannettoni, “A simplified model for zinc oxide surge arresters,” *IEEE Trans. Power Del.*, vol. 14, no. 2, pp. 393-398, Apr. 1999.

[20] IEC 60071-2, Insulation co-ordination – Part 2: Application guide, 1996.

[21] Joint Working Group 33/23.12, “Insulation co-ordination of GIS: Return of experience, on site tests and diagnostic techniques,” *Electra*, no. 176, pp. 67-97, Feb. 1998.

[22] P. N. Mikropoulos, T. E. Tsovilis, Z. G. Datsios, and N. C. Mavrikakis, “Effects of simulation models of overhead transmission line basic components on backflashover surges impinging on GIS substations,” in *Proc. 45th UPEC*, Cardiff, Wales, 2010, paper no. 72.